Digest Journal of Nanomaterials and Biostructures Vol. 12, No. 1, January - March 2017, p. 185 - 193

NANOCOMPOSITES OF ZnO AND TiO_2 HAVE ENHANCED ANTIMICROBIAL AND ANTIBACTERIAL PROPERTIES THAN THEIR DISJOINT COUNTERPARTS

C. S. CHAKRA[a], K. V. RAO[b], V. RAJENDAR[c*]
[a]*Centre for Nanoscience and Technology, Institute of Science and Technology, Jawaharlal Nehru Technological University Hyderabad, Telangana State,500085, India.*
[b]*School of Medicine, Radiology department, Johns Hopkins University, USA.*
[c]*Department of Electronics Engineering, Yeungnam University, Gyeongsan 38541, South Korea.*

Nanocomposites of inorganic oxides such as zinc oxide and titanium dioxides have shown to have greater synergistic effects in terms of their physiochemical properties. In this study we describe the antibacterial and anticancer activities of a nanocomposite prepared by combining zinc oxide and titanium dioxide nanoparticles. X-ray diffraction, Field emission scanning electron microscopy, transmission electron microscopy, Fourier transform infrared spectroscopy and dynamic light scattering techniques were used to analyze the samples. Then the samples at different molar ratios were analyzed for their antibacterial activities and anticancer activities on both gram positive and gram negative bacteria and four different cell lines respectively. The results indicate a greater efficacy on both antibacterial and anticancer properties compared to their individual oxides.

(Received December 3, 2016; Accepted February 27, 2017)

*Keywords:*Nanocomposite; Zinc oxide; Titanium dioxide; Nanoparticles; Anticancer; Antibacterial

1. Introduction

Nanocomposites (NCs) made from the mixture of various nanoparticles (NPs) make up the fascinating world of material science [1-2] which have modified a significant portion of our daily lives [3-5]. Nanocomposite mixtures of individually prepared nanoparticles combined at different concentrations [6] as opposed doping [7] or substitution [8-9] perform at a comparatively better scale in multiple applications. A lot of study has been done in this regard and have shown similar synergistic results [10-11]. The use of two different drugs instead of one is a common sight in medical applications [12], similarly, the use of multiple oxides instead one can be beneficial for biological and biochemical applications [13-14].

In this study, we have used zinc oxide nanoparticles (ZnO NPs) and titanium dioxide nanoparticles (TiO_2 NPs) as a nanocomposite to induce potent antibacterial and anticancer activities at millimolar concentrations [15-18]. In earlier studies, we have shown extensive antibacterial and anticancer activities of ZnO NPs and TiO_2 NPs [8-9]. Tween 80 was used as the surfactant in these experiments to control the shape and sizes have shown the most beneficial results [18-19]. Hence in this study, we have combined ZnO NPs and TiO_2 NPs via TWEEN 80 surfactant method and observed their antibacterial and anticancer properties through zone of inhibition (ZOI) and MTT assays.

*Corresponding author: rajendar.nano@gmail.com

2. Materials and Methods

2.1 Synthesis of ZnO/TiO_2 NCs

The preparation of the ZnO NPs and TiO_2 NPs is similar to those we have reported earlier [18-19]. In a typical procedure adopted for the preparation of ZnO/TiO_2 NCs, calculated amounts of ZnO NPs and TiO_2 NPs were mixed, and milled together using a mechanical milling machine (REMI, planetary ball 100 PM) at 400 revolutions per minute (rpm). The milling was performed for all the samples for 1 hr in stainless steel container using stainless steel balls of 2 mm diameter. The weight ratio of balls to the powder was maintained at 10:1 for all the samples and the samples were sintered at 250°C. The synthesized ZnO/TiO_2 NCs(1:1, 1:2, 1:3, 2:1, 2:3, 3:1, 3:2 wt%) were named as ZT1, ZT2, ZT3, ZT4, ZT5, ZT6 and ZT7.

2.2 Characterization Techniques

The prepared individual NPs and the NCs were analyzed by field emission scanning electron microscopy & energy dispersive spectroscopy (FESEM & EDS) and JEOL JEM-2010 (HT) transmission electron microscopy (TEM) to understand morphology and particle size. Dynamic light scattering (DLS) was performed on samples suspended in ethanol using a YD-laser (532 nm) and the mean value of the obtained histogram was considered the average particle size. Fourier transform infrared spectroscopy (FTIR) was performed for wavelengths 500-3700 cm-1. X-ray diffraction studies were performed between 2θ values 15° and 75°. The samples were then analyzed for their average crystallite size using the modified Scherrer's formula.

2.3 Antibacterial assay

Standard disc diffusion assay method was used for evaluating the antibacterial properties of the NCs [19-20]. As prototypical gram negative and gram positive *E.Coli, S. Aureus, B. Subtilis* and *C. Albicans* were used. Antibacterial results of ZnO/TIO_2 (1:1 wt%) NCs with concentrations of 0.025, 0.05, 0.75, 0.1, 0.125 and 0.15 mg/µl are studied with respect to antibiotic as reference.

2.4 Anticancer activity

MTT assay on four different cell lines - human cervical cancer cell line (HeLa), Chinese hamster ovary cells (CHO), human breast adenocarcinoma cell line (MD-231) and Mus musculus skin melanoma cell line (B16-F10) were used to show typical anticancer properties of the NCs. A 96-well plate with seating density of 2×10^4 per well were plated for individual cell lines and left overnight until they were 70% confluent. The noted concentrations (5, 25, 50, 75, 100 mg/µl) and control (PBS) were incubated with the cells for a period of 24 h at 37°C and 5% CO_2. A PBS wash was conducted twice on the cells and they were incubated with 200 µL of 1mg/µL MTT (3-(4,5-dimethylthiazol-2-yl)-2,5-diphenyltetrazolium bromide) for a period of 5 hours. Formazan crystals were dissolved using acidified isopropanol (0.1% Tris HCl in isopropanol) and transferred to a new 96 well plate. A Plate reader at 562 nm was used to quantify the MTT results. All the above experiments were conducted in triplicates and individually repeated 3 times to compensate for pipetting errors.

3. Results and discussions

3.1 Structural Analysis of ZnO/TiO_2 NCs

Figure 1 shows the XRD pattern of ZnO/TiO_2 NC with increasing TiO_2 wt%. Also we can observe that Anatase peaks of TiO_2 at 25°. The XRD peaks positions of ZnO and TiO_2 are well matched with standard JCPDS card numbers 36-1451 and 89-4921 respectively. Each peak having different 2θ positions corresponding to crystalline planes (hkl). The average crystallite sizes for these samples were analyzed by Debye Scherrer's formula ($D = K * \lambda/(\beta \cos \theta)$). β is the full width half maximum (FWHM) of the XRD corresponding peaks, K is Debye–Scherer's constant, D is crystallite size, λ is wave length of the X-ray, θ is Bragg angle. The average Crystallite size of ZT1, ZT2, ZT3, ZT4, ZT5, ZT6 and ZT7 NCs were found to be 15.3, 18.5, 19.8, 18, 22.2, 20.3, 25 nm respectively.

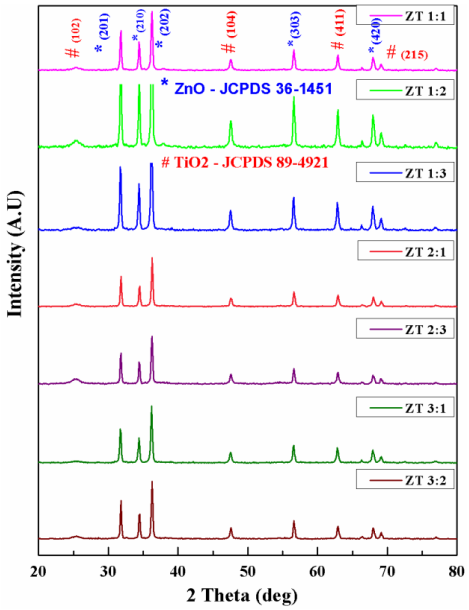

Fig 1. XRD pattern of ZnO/TiO_2 NC at different wt%

3.2 Morphology and particle size analysis

ZnO/TiO_2 NC (1:1wt%) morphological studies examined by FESEM, TEM and DLS. FESEM images of ZnO/TiO_2 NC indicates glouble like particles along with unstructured particles present in the sample shown in Fig.2(a-b). The TEM results complimentary for SEM results that an equal quantity of glouble shaped particles with variable particles shown in Fig.2(d-g). Energy dispersive x-ray spectroscopy (Fig.2(c)) confirms the ZnO NPs while unstructured particles were TiO_2, which confirms the FESEM results. The glouble shaped particles were confirmed to be ZnO NPs while unstructured particles were shown to be TiO_2 NPs shown in Fig.2(d-g). Fig.2(h)shows dynamic light scattering results, It is fascinating to note that the results revealed the particle size found to be 26 nm which the values are very close to those TEM observations.

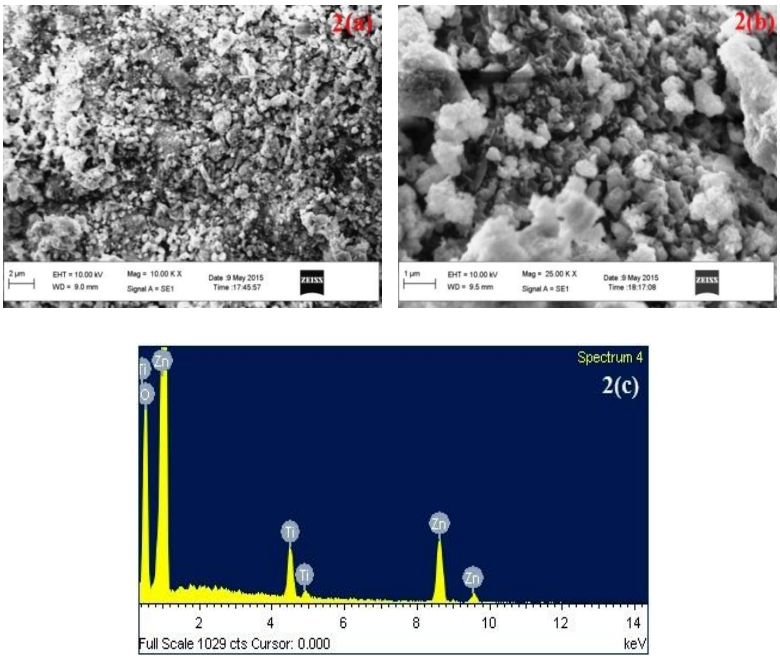

Fig2(a-c): FESEM Images of ZnO/TiO_2 NC (1:1) at 2 µm, 1 µm magnifications and it's EDS spectrum

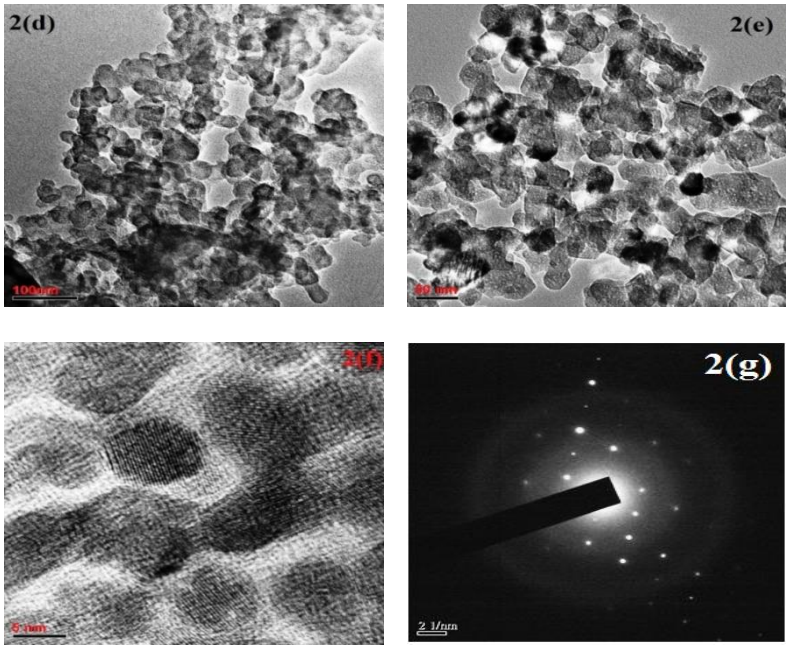

Fig 2(d-g): TEM images of ZnO/TiO_2 NC (1:1) at 100 nm, 50 nm, 5 nm magnification and it's SAED pattern

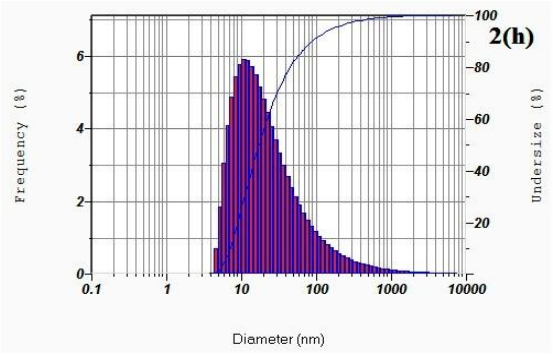

Fig 2(h): Particle size distribution of ZnO/TiO_2 NC (1:1)

3.3 Fourier Transform Infrared Spectroscopy (FTIR) analysis

Different weight percentages (1:1, 1:2, 1:3, 2:1, 2:3, 3:1 and 3:2 wt%) of ZnO/TiO_2 NC FTIR spectra recorded from wavelength range 500 to 3700 cm-1 shown in fig.3. Ti-O bonding is confirmed by broad absorption at ow frequency at 505 cm^{-1}. similarly C-O stretching is observed at 1199 cm^{-1}, C-C stretching at 1466 cm^{-1} C=C stretching at 1692 and 1735 cm^{-1}. And the Zn-O bonding observed at 2854, 2957 cm^{-1} and O-H stretching at 3502 cm^{-1}. Nearly same functional groups were observed in all samples.

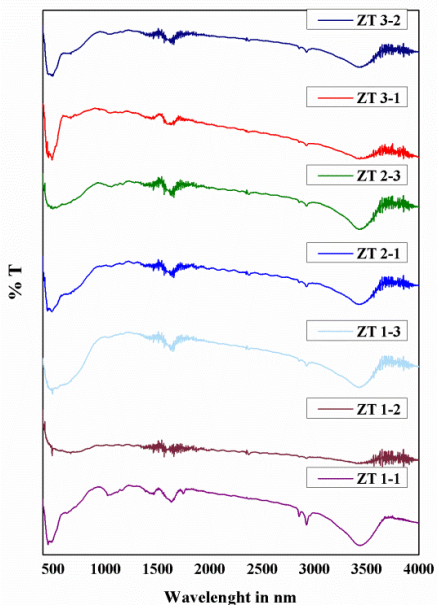

Fig 3. FTIR of ZnO/TiO_2 NC at different wt%

3.4 Antibacterial Assay

ZOI has been calculated for ZnO NPs, TiO_2 NPs and ZnO/TiO_2 NCs at different concentrations and the values are shown in table 1, 2, 3 and images shown in figure 4, 5, 6 and 7 with respect to control and antibiotic as references. Which confirms that ZnO NPs having some lower antibacterial activity than TiO_2 NPs. Because of the spontaneous mutation caused by TiO_2 NPs in bacterial samples as opposed to the ROS based mechanism explained for ZnO NPs. And the antibacterial activity of ZnO/TiO_2 NCs significantly increases compared to ZnO NPs alone and decreases to a small extent when compared to TiO_2 NPs. this is the important observation because, TiO_2 NPs are known to cause genetic mutations in human beings when applied in higher quantities as opposes to the biocompatible and non-toxic property of ZnO NPs. finally we can conclude that the use of ZnO/TiO_2 NCs would significantly improves the antibacterial activity of ZnO NPs while lowering the toxic range of TiO_2 NPs alone.

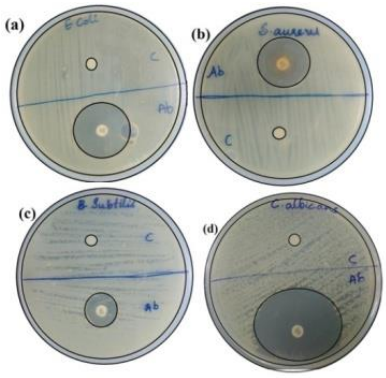

Fig 4: ZOI growths of (a) E. Coli (b) S. Aureus (c) B. Subtilis (d) C. Albicans with respect to Control & antibiotic

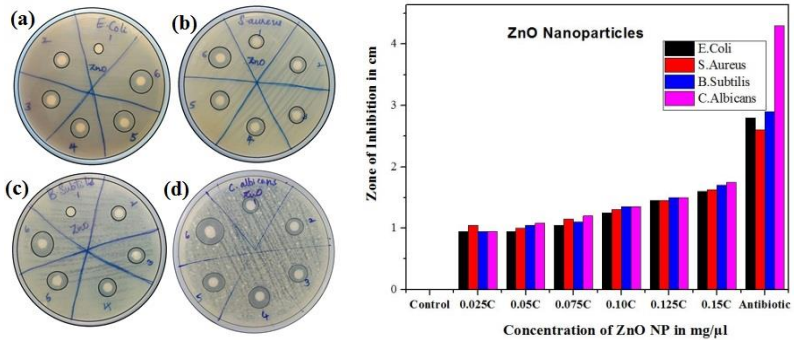

Fig 5 & Table 1: ZnO NPs ZOI growths of (a) E. Coli (b) S. Aureus (c) B. Subtilis (d) C. Albicans (Fig 5) and respective bar diagram of ZOI growths(Table 1)

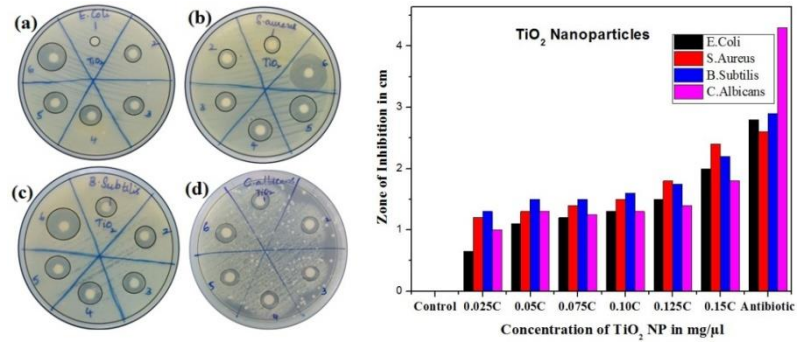

Fig 6 & Table 2: TiO_2 NPs ZOI growths of (a) E.Coli (b) S. Aureus (c) B. Subtilis (d) C. Albicans (Fig 6) and respective bar diagram of ZOI growths (Table 2)

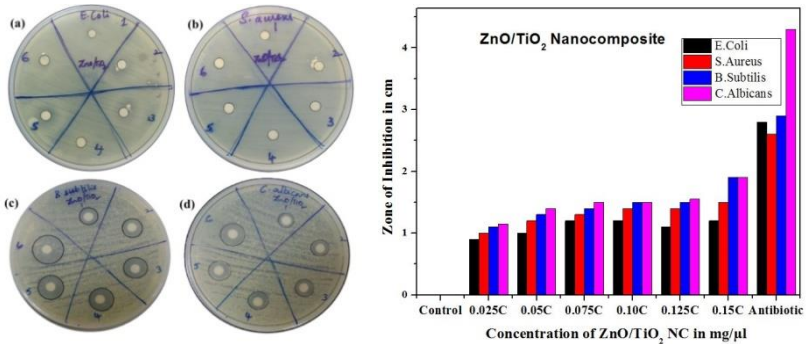

Fig 7 & Table 3: ZnO/TiO_2 NCs ZOI growths of (a) E. Coli (b) S. Aureus (c) B. Subtilis (d) C. Albicans (Fig 7) and respective bar diagram of ZOI growths (Table 3)

3.5 Anticancer activity

Similar to the antibacterial activity, the MTT assay was performed for ZnO NPs, TiO_2 NPs and ZnO/TiO_2 NCs shown in figure 8(a-c) and Table 4. The anticancer activity of ZnO NPs alone having lower activity than TiO_2 NPs which is complimentary to antibacterial activity. This would mean that a composite material would significantly alter the methodology through which anticancer activities could be governed without compromising on the biocompatibility issues. From these studies we can observe that TiO_2 NPs alone having the lower anticancer activity than ZnO NPs alone except for CHO cell line. In addition, the anticancer activity of ZnO NPs shows lower activity against CHO cell lines than other cell lines. But anticancer activity of ZnO/TiO_2 NCs shows significantly high and equivalent against all the cell lines. This confirms that through

the use of nanocomposites, the disadvantages offered by one particle can be compensated by the other particle used in the sample.

Table 4: Percentage of cell viability - bar diagram for ZnO NPs, TiO_2 NPs and ZnO/TiO_2 NC against HeLa, CHO, MD-231, B-16F10 cancer cells

	% Cell Viability											
Concentration in µg/µL	**HeLa cells**			**CHO cells**			**MD-231 cells**			**B-16F10 cells**		
	ZnO NP	**TiO_2 NP**	**ZnO/ TiO_2 NC**	**ZnO NP**	**TiO_2 NP**	**ZnO/ TiO_2 NC**	**ZnO NP**	**TiO_2 NP**	**ZnO/ TiO_2 NC**	**ZnO NP**	**TiO_2 NP**	**ZnO/ TiO_2 NC**
Control	100	100	100	100	100	100	100	100	100	100	100	100
1	84.3	94.33	87.87	94.33	92.78	90.08	87.87	94.34	87.87	47.52	87.82	85.84
25	73.25	89.56	84.3	92.78	87.82	85.84	68.52	82.64	68.52	36.86	81.85	74.45
50	50.88	78.45	66.82	89.85	81.85	67.86	56.87	67.61	56.87	27.09	68.52	44.85
75	27.09	52.22	45.49	90.08	54.89	47.52	23.18	66.82	23.18	23.18	56.87	36.86
100	19.0	29.08	36.51	87.87	23.18	35.1	17.27	50.88	17.1	17.27	36.51	28.85

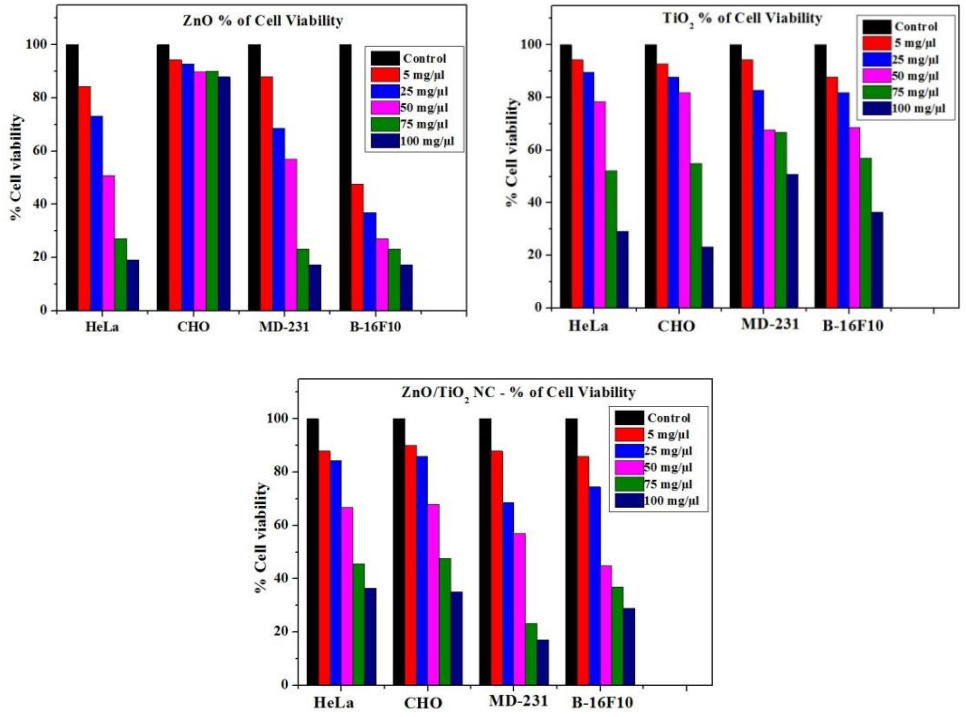

Fig 8(a-c): Percentage of cell viability for ZnO NPs (Fig.8(a)), TiO_2 NPs (Fig.8(b)) and ZnO/TiO_2 NC (Fig.8(c)) against HeLa, CHO, MD-231, B-16F10 cancer cells

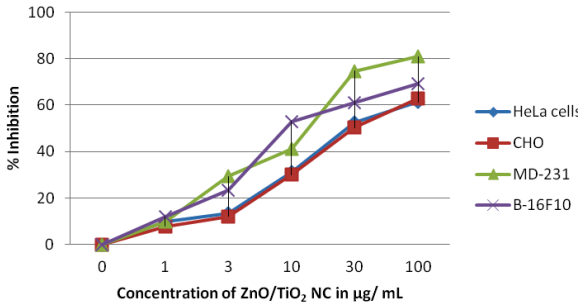

Fig 8(d): Percentage of inhibition Vs Concentration of ZnO/TiO_2 NC in mg/µl against cancer cells

This implies that through the use of nanocomposites, the disadvantages offered by one particle can be compensated by the other particle used in the sample. This would imply that a composite material would fundamentally modify the procedure through which anticancer exercises could be represented without bargaining on the biocompatibility issues. One more important observation from these studies is that TiO_2 NPs showed lower anticancer activity than ZnO NPs for all concentrations except for CHO cell line. In any case, anticancer activity is significantly high and equivalent for ZnO/TiO_2 NCs against all cell lines. This implies that through the use of nanocomposites, the disadvantages offered by one particle can be compensated by the other particle used in the sample.

4. Conclusions

The nanocomposites of zinc oxide and titanium dioxide mixture had elevated antibacterial property when compared to their individual counterparts. However, lower anticancer property was seen for the nanocomposite when compared to zinc oxide. But the nanocomposites had a greater anticancer property in case of the nanocomposite when compared to titanium dioxide. The bacterial types and cancer cell lines which responded much more efficiently for the composite rather than the individual nanoparticles in general. So this concludes the hypothesis that the use of synergistic compounds can indeed elevate antibacterial and anticancer responses. Future studies using much more complex nanocomposite mixtures will give us a better idea as to what combination of nanoparticles could be used for the best results.

Acknowledgment

The authors are graceful to Prof. CH. Sasikala, Centre for Environment, Institute of Science and Technology, JNT University Hyderabad, India, for providing the research facilities to undertake this work.

References

[1] F.J. Heiligtag, M. Niederberger, Materials Today. **16**(7,8) 262 (2013).
[2] K.S. Hougaarda, L. Campagnolob, P.C. Palmer, Reproductive Toxicology. **56**, 118 (2015).
[3] P.T. Biyela, J. Lin, C.C. Bezuidenhout, Water Science & Technology.**50**(1),45 (2004).
[4] S. Huang, L. Wang, L. Liu, Y. Hou, L. Li, Agron Sustainable Dev. **35**(2), 369 (2015.
[5] M Liu, Q. Chen, C. Lai, Y. Zhang, J. Deng, H. Li, S. Yao, Biosensors and Bioelectronics **48**(15), 75(2013).
[6] V. Rajendar, K.V. Rao, M. Ahmadipour, K. Shoban, Advanced Science, Engineering and Medicine. **05**(11), 1176 (2013).

[7] V. Rajendar, T. Dayakar, K. Shobhan, I. Srikanth, K.V. Rao, SuperlatticesMicrostruct. **75**, 551(2014).
[8] V. Rajendar, K.V. Rao, M. Ahmadipour, K. Shoban, Advanced Science, Engineering and Medicine.**05**(11)1176 (2013).
[9] V. Rajendar, N.P. Raju, K.V. Rao, **5**, 683 (2014).
[10] E. Flahaut, A. Peigney, C. Laurent, C. Marlière, F. Chastel, A. Rousset, Acta Mater. **48**(14), 3803 (2000).
[11] C.G. Granqvist, Mater SciEng A. **168**(2), 209 (1993).
[12] E.R. Arakelova, S.G. Grigoryan, F.G. Arsenyan, N.S. Babayan, R.M. Grigoryan, N.K. Sarkisyan, International Journal of Medical, Health, Biomedical, Bioengineering and Pharmaceutical Engineering. **8**(1), 33 (2014).
[13] H. Hurwitz, L. Fehrenbacher, W. Novotny, T. Cartwright, J. Hainsworth, W. Heim, et al. New Engl J Med. **350**(23), 2335 (2004).
[14] H. Chen, M. Zhang, B. Li, D. Chen, X. Dong, Y. Wang, Y. Gu, Biomaterials. **53**, 532 (2015).
[15] Y. Ding, L. Zhou, X. Chen, Q.Wu, Z. Song, S. Wei, J. Zhou, J. Shen, International Journal of Pharmaceutics.**498**(1-2), 335 (2016).
[16] L. Brunet, D.Y. Lyon, E.M. Hotze, P.J.J. Alvarez, M.R. Wiesner, Environ Sci Technol. **43**(12), 4355 (2009).
[17] N. Tyagi, S.K. Srivastava, S. Arora, Y. Omar, ZM. Ijaz et.al Cancer Letters. **383**(1), 53 (2016).
[18] V. Rajendar, Ch. Shilpa Chakra, B. Rajitha, K.V. Rao, M.C.Sekhar, B.P. Reddy, et al. J Mater Sci Mater Electron. **28**(4) 3272 (2017).
[19] V. Rajendar, CH. Shilpa Chakra, B. Rajitha, K.V. Rao, S. Park. J Mater Sci Mater Electron. **28**(4) 3294 (2017).